Osteoporotic bone of miR-150-deficient mice: Possibly due to low serum OPG-mediated osteoclast activation

Sik-Won Choi [a,1], Su Ui Lee [b,1], Eun Hye Kim [a], Sang-Joon Park [c], Inpyo Choi [d,e], Tae-Don Kim [d,e,*], Seong Hwan Kim [a,**]

[a] Laboratory of Translational Therapeutics, Korea Research Institute of Chemical Technology, Daejeon 305-600, Republic of Korea
[b] Natural Medicine Research Center, Korea Research Institute of Bioscience and Biotechnology, Cheongju-si, Chungbuk 363-883, Republic of Korea
[c] Department of Histology, College of Veterinary Medicine, Kyungpook National University, Daegu 702-701, Republic of Korea
[d] Immunotherapy Research Center, Korea Research Institute of Bioscience and Biotechnology, Daejeon 305-806, Republic of Korea
[e] Department of Functional Genomics, Korea University of Science and Technology, Daejeon 305-333, Republic of Korea

ARTICLE INFO

ABSTRACT

MicroRNA (miR)-150 has been shown to control B and T cell differentiation in the bone marrow. The regulation of B and T cells is directly or systematically associated with bone remodeling cells such as osteoclasts; however, the functional role of miR-150 in bone homeostasis has not been well studied. Here, we observed down-regulation of miR-150 during in vitro osteoclast differentiation and, furthermore, that miR-150 knockout mice exhibit decreased bone mass and an increased number of osteoclasts. miR-150 deficiency did not affect osteoclast differentiation, but miR150 knockout mice had significantly lower osteoprotegrin (OPG) serum levels, suggesting that the reduction of serum OPG level in miR-150 knockout mice might induce B cell expansion and subsequently increase serum levels of immunoglobulins for activating osteoclast differentiation.

1. Introduction

MicroRNAs (miRNAs) are evolutionarily conserved small non-coding RNAs that post-transcriptionally repress target genes by binding their 3′ untranslated regions. In maintaining bone homeostasis, miRNAs regulate the differentiation of bone precursor cells into osteoclasts and function of mature osteoclasts in a cell-restricted and/or paracrine/endocrine manner (Gamez et al., 2014; van der Eerden, 2014). In a previous study, 9 miRNAs were clinically identified as being up-regulated in the serum of osteoporosis patients, and 6 miRNAs exhibited significantly higher expression in the bone tissue of osteoporotic patients (Seeliger et al., 2014).

The aberrant in vivo biogenesis of miRNAs consequently leads to an imbalance of bone remodeling due to the over-activation and/or increased number of bone resorptive osteoclasts, resulting in low bone density, a state by which bone-related disorders such as osteoporosis, rheumatoid arthritis and cancer are characterized (van Wijnen et al., 2013; Papaioannou et al., 2014). Basically, hematopoietic stem cells (monocytes and bone marrow-derived macrophages, BMMs) differentiate into multinucleated osteoclast cells (MNCs) accompanied by the induction of tartrate-resistant acid phosphatase (TRAP), a biomarker of osteoclast differentiation. The formation of TRAP-positive MNCs (TRAP$^+$-MNCs) is directly induced by two essential cytokines: macrophage colony-stimulating factor (M-CSF) and receptor activator of nuclear factor-κB ligand (RANKL) (Boyle et al., 2003). In particular, the binding of RANKL to its receptor RANK triggers the activation of signaling cascades for osteoclast differentiation, but the action of RANKL is modulated by a decoy receptor, osteoprotegrin (OPG) (Simonet et al., 1997).

Osteoclast differentiation is also complicatedly regulated by immune cells and their activation and/or the cytokines they produce, such that osteoclast activity can be deregulated by autoimmunity or high inflammation (Long & Humphrey, 2012). Because the immune and skeletal

systems are functionally interconnected through shared mechanisms and crosstalk (Takayanagi, 2007), an understanding of the osteo-immunological pathogenesis of bone-related diseases could be helpful for identifying novel therapeutic targets in miRNAs.

The importance of miR-150 in the maturation of immune cells has been reported in several studies (Xiao et al., 2007; Zhou et al., 2007; Bezman et al., 2011; Zheng et al., 2012), but its relevance to bone homeostasis has not been studied. In preliminary studies, we found that miR-150 expression was down-regulated during in vitro osteoclast differentiation. Therefore, in this study, we investigated the relevance of miR-150 to bone metabolism by determining whether miR-150 would affect morphological changes to bone in miR-150 knockout mice.

2. Materials and methods

2.1. Mice

Mice homozygous for the miR-150-knockout allele (miR-150$^{-/-}$) and wild-type C57/B6J were purchased from JAX Mice (Bar Harbor, ME), and identified by genotyping PCR according to the published protocol (http://www.jax.org). Animal care was performed in compliance with the Guide for the Care and Use of Laboratory Animals, from the Institute for Laboratory Animal Research at the Korea Research Institute of Bioscience and Biotechnology.

2.2. Preparation of mouse osteoclast precursor cells

The isolation of mouse BMMs and their differentiation into osteoclasts were carried out according to the guidelines of the Institutional Animal Care and Use Committee of the Korea Research Institute of Chemical Technology. BMMs were isolated as previously described (Choi et al., 2012). In detail, after cervical dislocation, bone marrow cells (BMCs) were obtained from 5-week-old male ICR mice (Damool Science, Daejeon, Korea) by flushing femurs and tibias with α-MEM supplemented with antibiotics (100 units/ml penicillin and 100 μg/ml streptomycin; Invitrogen Life Technologies, CA). BMCs were cultured on a culture dish in α-MEM supplemented with 10% fetal bovine serum (FBS; Invitrogen Life Technologies, CA) with 10 ng/ml of mouse recombinant M-CSF (R&D Systems, MN) for 1 day. Then, after non-adherent BMCs were replated on a Petri dish and cultured for 3 days in the presence of M-CSF (30 ng/ml), adherent BMMs were used for osteoclast differentiation.

2.3. Osteoclast differentiation

Isolated BMMs (1×10^4 cells/well in a 96-well plate or 3×10^5 cells/well in a 6-well plate) were seeded and cultured in the presence of the indicated concentration of mouse recombinant RANKL (R&D Systems, MN) and M-CSF (30 ng/ml) for 4 days to differentiate into mature MNCs.

2.4. TRAP staining and activity assay

Mature osteoclasts were visualized by TRAP staining. Briefly, MNCs were fixed with 3.7% formalin for 10 min, permeabilized with 0.1% Triton X-100 for 10 min, and stained with TRAP solution (Sigma-Aldrich, MO). TRAP$^+$-MNCs (≥3 nuclei) were counted. To measure TRAP activity, MNCs were fixed in 3.7% formalin for 5 min, permeabilized with 0.1% Triton X-100 for 10 min, and treated with a TRAP buffer (100 mM sodium citrate pH 5.0, 50 mM sodium tartrate) containing 3 mM p-nitrophenyl phosphate (Sigma-Aldrich, MO) at 37 °C for 5 min. Reaction mixtures in the wells were transferred to new plates containing an equal volume of 0.1 N NaOH and the optical density was determined at 405 nm.

2.5. RNA isolation and real-time polymerase chain reaction (PCR)

According to the manufacturer's protocols, total RNA was isolated with TRIzol reagent (Invitrogen Life Technologies, CA), and reverse transcription was performed with 1 μg of RNA using oligo(dT) primers, dNTP, RNase inhibitor and SuperScript II reverse transcriptase (Invitrogen Life Technologies, CA). For evaluating mRNA expression levels, SYBR green-based PCR was performed with the Stratagene Mx3000 Real-Time PCR system and Brilliant SYBR Green Master Mix (Stratagene, CA) as described previously (100). Table 1 lists the primers used in this study. GAPDH was used as an internal control. The miR-150 primers were purchased from Exiqon (MA). For evaluating the expression levels of miR-150, miR SYBR Green Master Mix (Exiqon, MA) was used according to the manufacturer's protocol. U6 primers were purchased from Exiqon, and used as an internal control for miRNA.

2.6. Western blot analysis

Cells were lysed in ice-cold lysis buffer (50 mM Tris–HCl, 150 mM NaCl, 5 mM EDTA, 1% Triton X-100, 1 mM sodium fluoride, 1 mM sodium vanadate, and 1% deoxycholate) supplemented with 1 mM phenylmethylsulfonyl fluoride (PMSF; BIO BASIC Inc., CA). The lysates were centrifuged at 12,000 ×g for 10 min. The protein concentration in the supernatant was determined using the DC protein assay kit (Bio-Rad, CA) according to the manufacturer's protocol. Proteins (20 μg) were boiled in sodium dodecyl sulfate (SDS) sample buffer for 5 min, separated in an 8% SDS-polyacrylamide electrophoresis gel and transferred onto a polyvinylidene difluoride membrane (Amersham Biosciences, NJ). The membrane was preincubated at room temperature with 5% skim milk in TBST (0.1% Tween 20 in Tris-buffered saline) for 1 h, probed with a primary antibody against NFATc1 or actin (Santa Cruz Biotechnology, TX), and incubated overnight at 4 °C. The membrane was washed with TBST three times for 30 min and then incubated at room temperature with a horseradish peroxidase-conjugated secondary antibody (Santa Cruz Biotechnology, TX) for 2 h. After washing with TBST, the immunoblotting signals were detected using the Super-Signal West Pico Chemiluminescent Substrate (Pierce Chemical Co., IL) with an LAS-3000 luminescent image analyzer (Fuji Photo Film Co., Japan).

2.7. Micro-computed tomography (μCT) and histological analysis

Bone histomorphometric analyses were performed in Genoss Co. (Korea) with a μCT scanner (SkyScan1173, Bruker Corporation, Germany), and the images were obtained using DataViewer (SKYSCAN). All histomorphometric parameters were described in accordance with standard criteria (Dempster et al., 2013; Bouxsein et al., 2010). Femurs were fixed in 4% paraformaldehyde in phosphate buffered saline (PBS) overnight, decalcified in 12% EDTA, hydrated, paraffin-embedded, sectioned, and stained with hematoxylin and eosin (H&E) and the TRAP solution kit (Sigma-Aldrich, MO).

2.8. Enzyme-linked immunosorbent assay (ELISA)

Blood serums were collected from the infraorbital venous plexus of mice (13-week-old, male, n = 7) using a heparinized capillary tube

Table 1
Primer sequences used in this study.

Target gene	Forward (5′-3′)	Reverse (5′-3′)
c-Fos	CTGGTGCAGCCCACTCTGGTC	CTTTCAGCAGATTGGCAATCTC
NFATc1	GGGTCAGTGTGACCGAAGAT	GGAAGTCAGAAGTGGGTGGA
TRAP	ACTTCCCCAGCCCTTACTAC	TCAGCACATAGCCCACACCG
GAPDH	ACCACAGTCCATGCCATCAC	TCCACCACCCTGTTGCTGTA

(Paul Marienfeld, Germany). Cytokines in blood serum were quantified by an ELISA assay. ELISA kits for RANKL or OPG quantification were obtained from Abcam (MA). ELISA kits for tumor necrosis factor (TNF)-α, and interferon (IFN)-γ quantification were obtained from R&D Systems (MN). Assays were performed according to the manufacturers' protocol.

2.9. Statistical analysis

All quantitative values are presented as the mean $\pm$ standard deviation (SD). Significant differences were analyzed using Student's t-test. A value of $P < 0.05$ was considered statistically significant.
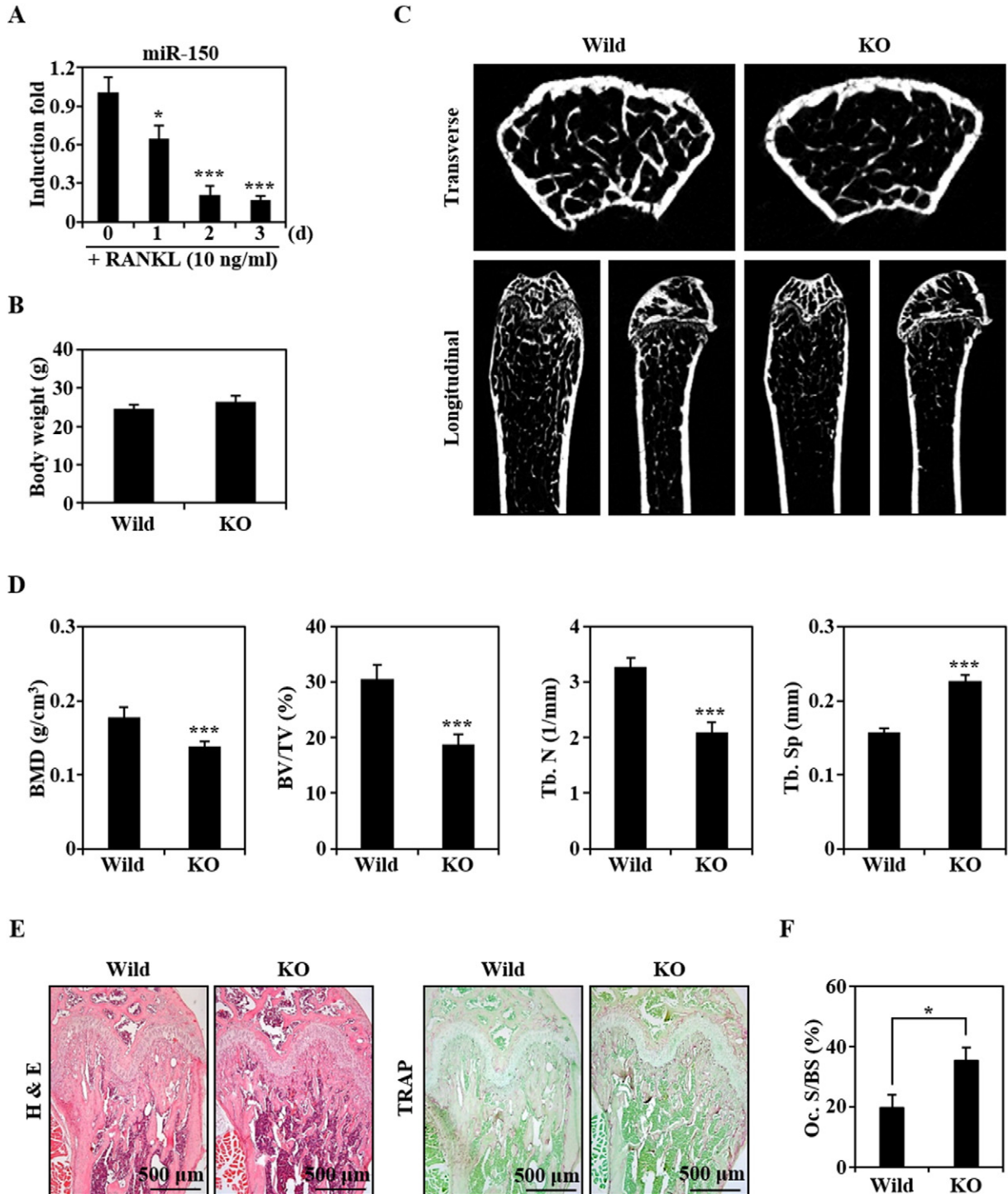

Fig. 1. miR-150 is down-regulated during osteoclast differentiation and its knockout mice exhibit a decreased bone mass with an increased number of osteoclasts. (A) The expression levels of miR-150 during RANKL-induced osteoclast differentiation were evaluated by real-time PCR. The relative induction fold of miR-150 is presented. * $P < 0.05$; *** $P < 0.001$, vs. 0 day. (B) Body weights of the wild-type and miR-150 knockout mice (KO; 13-week-old male, n = 5) were measured. (C) Transverse and longitudinal images of the proximal left femurs isolated from the wild-type and miR-150 knockout mice were generated by μCT. (D) BMD, BV/TV, Tb.N, and Tb.Sp of femurs (n = 5) were analyzed using an μCT scanner and CTAn software. *** $P < 0.001$, vs. the wild type. (E) Histological analysis was performed by H&E and TRAP staining. (F) The osteoclast surface per bone surface (Oc. S/BS) was measured by imageJ. *$P < 0.05$, vs. the wild type.

3. Results and discussion

3.1. miR-150 is down-regulated during osteoclast differentiation and mir-150 knockout mice exhibit decreased bone mass with an increased number of osteoclasts

Several miRNAs have been reported to regulate osteoclast differentiation (Xia et al., 2011; Kagiya & Nakamura, 2013). Here, we are the first to report that miR-150 expression is gradually down-regulated during RANKL-mediated differentiation of normal BMMs into osteoclasts (Fig. 1A).

As reported previously (Xiao et al., 2007), miR-150 knockout mice are viable, fertile, and morphologically normal. In the current study, there were no differences in body weight between wild-type and miR-150 knockout mice (Fig. 1B), but μCT analysis revealed that trabecular bone mineral density (BMD), bone volume/tissue volume (BV/TV or bone volume fraction), and the number of trabeculae (Tb.N) in femurs were significantly lower, and that trabecular separation (Tb.Sp) greater, in miR-150 knockout mice, suggesting that miR-150-deficiency is phenotypically osteoporotic (Fig. 1C and D). This suggestion was confirmed in H&E-stained and TRAP-stained histological sections showing lower trabecular density and increased numbers of TRAP-stained osteoclasts in miR-150 knockout mice compared to the wild type (Fig. 1E and F). In the subsequent experiments, we focused on the relevance of miR-150 to the formation of osteoclasts.

3.2. Osteoclast differentiation of isolated BMMs is similar in miR-150 knockout and wild-type mice

In BMMs isolated from miR-150 knockout mice, the expression levels of miR-150 were dramatically lower than those in wild-type mice (Fig. 2A). However, when miR-150$^{-/-}$ BMMs differentiated into osteoclasts, TRAP$^+$-MNCs were normally formed as observed in wild type (Fig. 2B). No difference was observed in the formation of TRAP$^+$-MNCs between wild-type and miR-150 knockout mice, nor was there a difference in osteoclast differentiation as confirmed by counting the TRAP$^+$-MNCs (Fig. 2C) and measuring TRAP activity (Fig. 2D). miR-150 has been reported to regulate the cell fate of megakaryocyte-erythroid progenitors (Lu et al., 2008) and its deficiency resulted in the defective development of natural killer (NK) and invariant NK T (iNKT) cells (Bezman et al., 2011; Zheng et al., 2012). miR-150 deficiency also reduced the capacity of Langerhans cells (LCs) for cross-presentation, but it did not interrupt the development, maturation, migration or phagocytic capacity of LCs (Mi et al., 2012). The findings of our study suggest that miR-150 deficiency has no functional relevance for the ability of precursors to differentiate into osteoclasts in in vitro conditions.

3.3. miR-150 knockout mice have significantly low serum levels of OPG, but not RANKL, IFN-γ or TNF-α

As well as no difference in the thickness of cortical bone between wild-type and miR-150 knockout mice (Supplementary Fig. 1), the in vitro results showing that the retroviral over-expression of miR-150 did not affect either osteoclast or osteoblast differentiation (Supplementary Fig. 2 and 3), along with the observation that miR-150 had no functional relevance for the ability of precursors to differentiate into osteoclasts in in vitro conditions, prompted us to further investigate mir-150's effect on the serum levels of in vivo systematic factors such as OPG, RANKL, IFN-γ and TNF-α. As shown in Fig. 3, miR-150 knockout mice had significantly lower serum levels of OPG, but not of RANKL, IFN-γ or TNF-α.
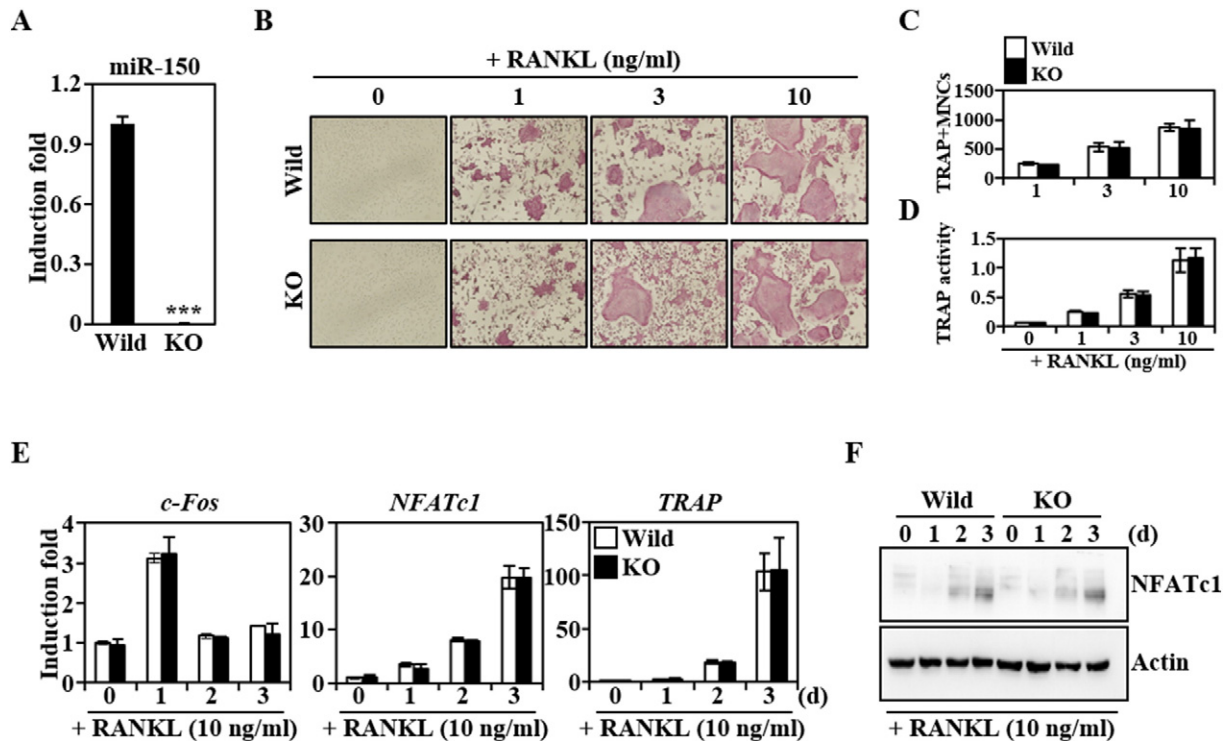

Fig. 2. Osteoclast differentiation of BMMs isolated from miR-150 knockout mice was similar to that of the wild type. (A) The expression levels of miR-150 in BMMs isolated from the wild-type or miR-150 knockout mice (KO) were evaluated by real-time PCR. The relative induction fold of miR-150 is presented. BMMs were cultured with M-CSF (30 ng/ml) for 2 days, subsequently miR-150 expression levels were analyzed. *** $P < 0.001$, vs. the wild type. The effects of miR-150 deficiency on the formation of TRAP + −MNC (B, C), TRAP activity (D), mRNA levels of genes related to osteoclast differentiation (E) and NFATc1 protein expression (F) were evaluated. Briefly, isolated BMMs were cultured for 4 days in the presence of the indicated RANKL and M-CSF (30 ng/ml), and stained with a TRAP solution, and then photographed under a light microscope (magnification ×100, B–D). For expression level evaluation, BMMs were cultured for the indicated days with M-CSF (30 ng/ml) and RANKL (10 ng/ml). The mRNA and protein expression were analyzed by real-time PCR and Western blot, respectively (E, F).
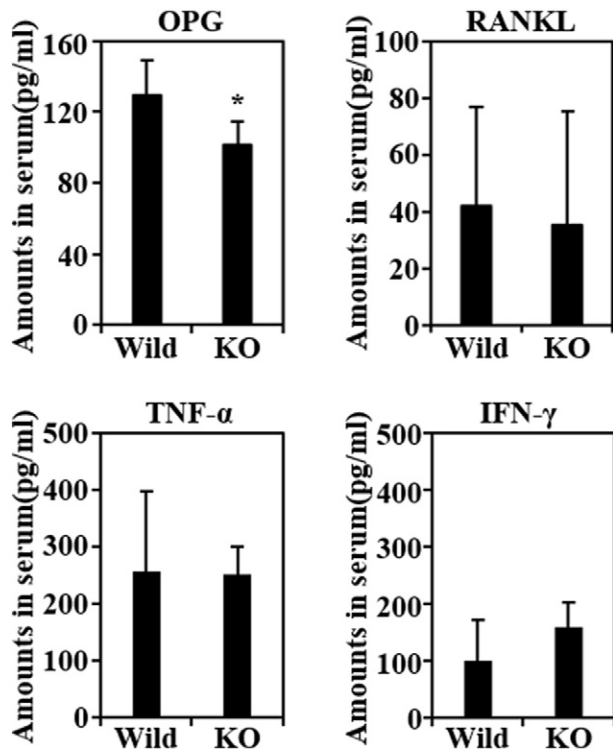
9

Fig. 3. miR-150 knockout mice had significantly lower serum levels of OPG, but not RANKL, IFN-γ or TNF-α. Serum levels of OPG, RANKL, TNF-α and IFN-γ were measured using ELISA assay kits as described in the Materials and methods section.

The physiological role of OPG in bone metabolism has been well established. OPG knockout mice display early-onset osteoporosis leading to large numbers of osteoclasts and severe bone destruction (Bucay et al., 1998). OPG production has been suggested to be attributable to B cells as well as to osteoblasts and their precursors (Li et al., 2007). Interestingly, HIV-induced B cell dysfunction leading to increased RANKL and decreased OPG has recently been reported to correlate with loss of BMD (Titanji et al., 2014), and B-cell knockout mice were shown to be deficient in OPG and osteoporotic (Li et al., 2007). However, considering the expansion of B1a cells in miR-150 knockout mice (Xiao et al., 2007), the positive relationship between B cell function and OPG levels may not explain the significantly lower serum levels of OPG in miR-150 mice.

Instead, we hypothesized that the reduction of OPG serum levels in miR-150-deficient mice might induce B cell expansion that subsequently increases serum levels of immunoglobulin (Ig) for activating osteoclast differentiation. Higher numbers of pro- and mature splenic B1 cells in OPG knockout mice have been reported (Yun et al., 2001). This could be consistent with B1a cell expansion in miR-150 knockout mice (Xiao et al., 2007). In addition, miR-150 deficiency resulted in higher serum Ig levels due to B1a cell expansion in the spleen and peritoneal cavity; miR-150 knockout mice exhibited a 9-fold increase in IgA, a 4-fold increase in IgG2b, a 3-fold increase in IgG1, and a 2-fold increase in IgM serum levels (Xiao et al., 2007). Considering that IgG autoantibody has been suggested to enhance osteoclast generation and bone destruction via its binding to select activating cellular fragment crystallizable (Fc)-γ receptors on immature osteoclasts (Seeling et al., 2013), OPG reduction in miR-150 deficiency might induce osteoclast differentiation via B cell expansion-mediated induction of IgG. In addition, the possibility that B1 cells differentiate into functional osteoclast-like cells cannot be excluded when explaining osteoporotic bone in miR-150 knockout mice (Pugliese et al., 2012). Furthermore, the activated B cells have been shown to enhance the osteoclastogenesis by expressing many osteoclastogenic factors (Choi et al., 2001).

T cells also induce B cell-mediated OPG production in vivo, and T-cell-deficient mice with diminished bone marrow OPG production were also osteoporotic (Li et al., 2007). However, conventional T cell development was normal under miR-150-deficient conditions (Zheng et al., 2012).

Activation of matured NK and iNKT cells was accompanied by the production of IFN-γ to inhibit osteoclast formation (Takahashi et al., 1986; Kamolmatyakul et al., 2001). In miR-150 knockout mice with impaired NK cell maturation, defective IFN-γ production has been observed (Bezman et al., 2011); compared to control, IFN-γ was produced by a significantly smaller proportion of miR-150$^{-/-}$ NK cells in response to in vitro stimulation. In addition, in vivo activated iNKT cells in miR-150$^{-/-}$ mice exhibited significantly higher production of IFN-γ (Zheng et al., 2012), however the amounts of IFN-γ produced by the controls and those by miR-150 knockout NK cells did not differ under no-stimulus conditions (Bezman et al., 2011). Consistent with this result, we observed no difference in IFN-γ serum levels between control and miR-150 knockout mice, suggesting that IFN-γ could not explain the osteoporotic bones of miR-150 knockout mice.

NK and iNKT cells have been shown to regulate osteoclast differentiation by their activation or production of RANKL (Soderstrom et al., 2010; Hu et al., 2011). It has been shown that NK cells are abundant in the inflamed joints of patients with rheumatoid arthritis (Soderstrom et al., 2010) and, conversely, that osteoporotic animals are characterized by a reduced number of NK cells and osteoclasts (Popoff et al., 1991; Roundy et al., 2003). In vivo activated iNKT cells promote the expansion of osteoclast precursors and lead to accelerated maturation and activation of osteoclasts; in addition, IFN-γ and TNF-α have been suggested to be negative and positive regulators of iNKT cell-induced osteoclast development (Hu et al., 2011). The impaired maturation of both cells has been reported in miR-150 deficiency (Bezman et al., 2011; Zheng et al., 2012), but we observed no difference in the serum levels of IFN-γ or TNF-α between the control and miR-150 knockout mice, suggesting that the osteoporotic bones of miR-150 knockout mice cannot be explained by the activity of NK and iNKT cells.

There are a lot of resources to produce OPG in the body. As well as bone, mouse OPG mRNA has been reported to be expressed in several tissues, including liver, lung, heart, kidney, stomach, intestines and skin (Simonet et al., 1997), and furthermore, in marrow, it is produced by a variety of cells, including stromal cells, B lymphocytes, and dendritic cells. In this study, serum OPG level was decreased in KO mice. Overexpression of miR-150 in osteoblasts did not change OPG levels. Then, which cells or tissues are responsible for the reduction of OPG in serum of miR-150 KO mice? Unfortunately, we have no idea or evidence to answer this question. This should be elucidated in a further study.

4. Conclusion

miR-150 expression was down-regulated during osteoclast differentiation, and miR-150 knockout mice exhibited decreased bone mass with an increased number of osteoclasts. Osteoclast differentiation of BMMs isolated from miR-150 knockout mice was similar to that of the wild type; however, miR-150 knockout mice had significantly lower serum levels of OPG, but not RANKL, IFN-γ or TNF-α. In miR-150 deficiency, the reduction of serum OPG levels may induce B cell expansion and subsequently increase serum levels of Igs that activate osteoclast differentiation.

Appendix A. Supplementary data

Supplementary data to this article can be found online at http://dx.doi.org/10.1016/j.bonr.2015.06.003.

References

Bezman, N.A., Chakraborty, T., Bender, T., Lanier, L.L., 2011. miR-150 regulates the development of NK and iNKT cells. J. Exp. Med. 208, 2717–2731.

Bouxsein, M.L., Boyd, S.K., Christiansen, B.A., Guldberg, R.E., Jepsen, K.J., Muller, R., 2010. Guidelines for assessment of bone microstructure in rodents using micro-computed tomography. J. Bone Miner. Res. 25, 1468–1486.

Boyle, W.J., Simonet, W.S., Lacey, D.L., 2003. Osteoclast differentiation and activation. Nature 423, 337–342.

Bucay, N., Sarosi, I., Dunstan, C.R., Morony, S., Tarpley, J., Capparelli, C., Scully, S., Tan, H.L., Xu, W., Lacey, D.L., Boyle, W.J., Simonet, W.S., 1998. osteoprotegerin-deficient mice develop early onset osteoporosis and arterial calcification. Genes Dev. 12, 1260–1268.

Choi, Y., Woo, K.M., Ko, S.H., Lee, Y.J., Park, S.J., Kim, H.M., Kwon, B.S., 2001. Osteoclastogenesis is enhanced by activated B cells but suppressed by activated CD8(+) T cells. Eur. J. Immunol. 31, 2179–2188.

Choi, S.W., Son, Y.J., Yun, J.M., Kim, S.H., 2012. Fisetin inhibits osteoclast differentiation via downregulation of p38 and c-Fos-NFATc1 signaling pathways. Evid. Based Complement. Alternat. Med. 2012, 810563.

Dempster, D.W., Compston, J.E., Drezner, M.K., Glorieux, F.H., Kanis, J.A., Malluche, H., Meunier, P.J., Ott, S.M., Recker, R.R., Parfitt, A.M., 2013. Standardized nomenclature, symbols, and units for bone histomorphometry: a 2012 update of the report of the ASBMR Histomorphometry Nomenclature Committee. J. Bone Miner. Res. 28, 2–17.

Gamez, B., Rodriguez-Carballo, E., Ventura, F., 2014. MicroRNAs and post-transcriptional regulation of skeletal development. J. Mol. Endocrinol. 52, R179–R197.

Hu, M., Bassett, J.H., Danks, L., Howell, P.G., Xu, K., Spanoudakis, E., Kotsianidis, I., Boyde, A., Williams, G.R., Horwood, N., Roberts, I.A., Karadimitris, A., 2011. Activated invariant NKT cells regulate osteoclast development and function. J. Immunol. 186, 2910–2917.

Kagiya, T., Nakamura, S., 2013. Expression profiling of microRNAs in RAW264.7 cells treated with a combination of tumor necrosis factor alpha and RANKL during osteoclast differentiation. J. Periodontal Res. 48, 373–385.

Kamolmatyakul, S., Chen, W., Li, Y.P., 2001. Interferon-gamma down-regulates gene expression of cathepsin K in osteoclasts and inhibits osteoclast formation. J. Dent. Res. 80, 351–355.

Li, Y., Toraldo, G., Li, A., Yang, X., Zhang, H., Qian, W.P., Weitzmann, M.N., 2007. B cells and T cells are critical for the preservation of bone homeostasis and attainment of peak bone mass in vivo. Blood 109, 3839–3848.

Long, C.L., Humphrey, M.B., 2012. Osteoimmunology: the expanding role of immunoreceptors in osteoclasts and bone remodeling. Bonekey Rep. 1.

Lu, J., Guo, S., Ebert, B.L., Zhang, H., Peng, X., Bosco, J., Pretz, J., Schlanger, R., Wang, J.Y., Mak, R.H., Dombkowski, D.M., Preffer, F.I., Scadden, D.T., Golub, T.R., 2008. MicroRNA-mediated control of cell fate in megakaryocyte–erythrocyte progenitors. Dev. Cell 14, 843–853.

Mi, Q.S., Xu, Y.P., Qi, R.Q., Shi, Y.L., Zhou, L., 2012. Lack of microRNA miR-150 reduces the capacity of epidermal Langerhans cell cross-presentation. Exp. Dermatol. 21, 876–877.

Papaioannou, G., Mirzamohammadi, F., Kobayashi, T., 2014. MicroRNAs involved in bone formation. Cell. Mol. Life Sci. 71, 4747–4761.

Popoff, S.N., Jackson, M.E., Koevary, S.B., Marks Jr., S.C., 1991. Coexistence of reduced function of natural killer cells and osteoclasts in two distinct osteopetrotic mutations in the rat. J. Bone Miner. Res. 6, 263–271.

Pugliese, L.S., Goncalves, T.O., Popi, A.F., Mariano, M., Pesquero, J.B., Lopes, J.D., 2012. B-1 lymphocytes differentiate into functional osteoclast-like cells. Immunobiology 217, 336–344.

Roundy, K., Smith, R., Weis, J.J., Weis, J.H., 2003. Overexpression of RANKL implicates IFN-beta-mediated elimination of B-cell precursors in the osteopetrotic bone of microphthalmic mice. J. Bone Miner. Res. 18, 278–288.

Seeliger, C., Karpinski, K., Haug, A.T., Vester, H., Schmitt, A., Bauer, J.S., van Griensven, M., 2014. Five freely circulating miRNAs and bone tissue miRNAs are associated with osteoporotic fractures. J. Bone Miner. Res. 29, 1718–1728.

Seeling, M., Hillenhoff, U., David, J.P., Schett, G., Tuckermann, J., Lux, A., Nimmerjahn, F., 2013. Inflammatory monocytes and Fcgamma receptor IV on osteoclasts are critical for bone destruction during inflammatory arthritis in mice. Proc. Natl. Acad. Sci. U. S. A. 110, 10729–10734.

Simonet, W.S., Lacey, D.L., Dunstan, C.R., Kelley, M., Chang, M.S., Luthy, R., Nguyen, H.Q., Wooden, S., Bennett, L., Boone, T., Shimamoto, G., DeRose, M., Elliott, R., Colombero, A., Tan, H.L., Trail, G., Sullivan, J., Davy, E., Bucay, N., Renshaw-Gegg, L., Hughes, T.M., Hill, D., Pattison, W., Campbell, P., Sander, S., Van, G., Tarpley, J., Derby, P., Lee, R., Boyle, W.J., 1997. Osteoprotegerin: a novel secreted protein involved in the regulation of bone density. Cell 89, 309–319.

Soderstrom, K., Stein, E., Colmenero, P., Purath, U., Muller-Ladner, U., de Matos, C.T., Tarner, I.H., Robinson, W.H., Engleman, E.G., 2010. Natural killer cells trigger osteoclastogenesis and bone destruction in arthritis. Proc. Natl. Acad. Sci. U. S. A. 107, 13028–13033.

Takahashi, N., Mundy, G.R., Roodman, G.D., 1986. Recombinant human interferon-gamma inhibits formation of human osteoclast-like cells. J. Immunol. 137, 3544–3549.

Takayanagi, H., 2007. Osteoimmunology: shared mechanisms and crosstalk between the immune and bone systems. Nat. Rev. Immunol. 7, 292–304.

Titanji, K., Vunnava, A., Sheth, A.N., Delille, C., Lennox, J.L., Sanford, S.E., Foster, A., Knezevic, A., Easley, K.A., Weitzmann, M.N., Ofotokun, I., 2014. Dysregulated B cell expression of RANKL and OPG correlates with loss of bone mineral density in HIV infection. PLoS Pathog. 10 (e1004497).

van der Eerden, B.C., 2014. MicroRNAs in the skeleton: cell-restricted or potent intercellular communicators? Arch. Biochem. Biophys. 561, 46–55.

van Wijnen, A.J., van de Peppel, J., van Leeuwen, J.P., Lian, J.B., Stein, G.S., Westendorf, J.J., Oursler, M.J., Im, H.J., Taipaleenmaki, H., Hesse, E., Riester, S., Kakar, S., 2013. MicroRNA functions in osteogenesis and dysfunctions in osteoporosis. Curr. Osteoporos. Rep. 11, 72–82.

Xia, Z., Chen, C., Chen, P., Xie, H., Luo, X., 2011. MicroRNAs and their roles in osteoclast differentiation. Front. Med. 5, 414–419.

Xiao, C., Calado, D.P., Galler, G., Thai, T.H., Patterson, H.C., Wang, J., Rajewsky, N., Bender, T.P., Rajewsky, K., 2007. MiR-150 controls B cell differentiation by targeting the transcription factor c-Myb. Cell 131, 146–159.

Yun, T.J., Tallquist, M.D., Aicher, A., Rafferty, K.L., Marshall, A.J., Moon, J.J., Ewings, M.E., Mohaupt, M., Herring, S.W., Clark, E.A., 2001. Osteoprotegerin, a crucial regulator of bone metabolism, also regulates B cell development and function. J. Immunol. 166, 1482–1491.

Zheng, Q., Zhou, L., Mi, Q.S., 2012. MicroRNA miR-150 is involved in Valpha14 invariant NKT cell development and function. J. Immunol. 188, 2118–2126.

Zhou, B., Wang, S., Mayr, C., Bartel, D.P., Lodish, H.F., 2007. miR-150, a microRNA expressed in mature B and T cells, blocks early B cell development when expressed prematurely. Proc. Natl. Acad. Sci. U. S. A. 104, 7080–7085.